

Investigation of universal small-scale structures in turbulence using Shake-The-Box Lagrangian Particle Tracking and FlowFit

Tom Buchwald¹, Daniel Schanz², Sebastian Gesemann² and Andreas Schröder^{1,2}

1: Brandenburg University of Technology Cottbus-Senftenberg, Institute of Traffic Engineering, Cottbus, Germany

2: German Aerospace Center (DLR), Institute of Aerodynamics and Flow Technology, Göttingen, Germany

* Correspondent author: Tom.Buchwald@b-tu.de

Keywords: 3D Velocity Gradient Tensor, turbulent energy dissipation rate, Lagrangian Particle Tracking, Shake-The-Box, FlowFit

ABSTRACT

A characteristic property of turbulent flows is the presence of a universal small-scale structure consisting of a shear layer separated by two stretched vortices. This pattern becomes visible by averaging the velocity sampled in the eigenframe of the local strain rate tensor. In this contribution, the structure is detected and tracked over time to investigate its formation and decay. For this purpose, experimental data of a von Kármán flow at $Re_\lambda = 370$ is used, which is analyzed with Shake-The-Box (STB) Lagrangian Particle Tracking (LPT) and the data assimilation method FlowFit. The universal structure is characterized by the time-resolved mean distribution of dissipation and pressure in the strain rate eigenframe. Using the average power balance terms along all particle trajectories passing through the direct vicinity of conditioned high-dissipation ($> 7.5 < \varepsilon >$) and enstrophy ($> 7.5 < \omega^2 >$) events during the time-span from $-4 \tau_\eta < t < 4 \tau_\eta$ the Lagrangian energy transport mechanism through such intermittent events can be discovered, at least in a mean sense. It is shown how the impact of the particles in a high dissipative event leads to a part of the energy being converted into heat and another part into rotation in a time period of approximately $2\tau_\eta$. This finding is consistent with the existence of the universal structure. Thus, a connection of Eulerian universal structures with their underlying energy exchange processes is proposed. Furthermore, instantaneous high dissipative events and the Lagrangian tracks that constitute them are shown and related to the statistical results.

1. Introduction

It is widely acknowledged that turbulent flows have some universal features. One of them is the preferential alignment of the second eigenvector $\vec{\lambda}_2$ of the strain rate tensor S with the vorticity vector $\vec{\omega}$. (Tsinober 2001) Another feature is the teardrop shape of the joint probability density function of the principal invariants of the velocity gradient tensor (Soria 1994), which indicates that turbulent flow consist mostly of stable foci and unstable node-saddle topologies (Chong et. al. 1990). It has been shown that averaging velocity fields obtained in local coordinate frames yield

an explanation for these features (Elsinga and Marusic 2010). As can be seen in Figure 1, the average flow pattern in the strain rate tensor eigenframe consists of a shear layer with two stretched vortices separating two regions of virtually uniform flow. This suggests that the alignment of $\vec{\lambda}_2$ and $\vec{\omega}$ as well as the teardrop shape of the Q-R-plot are actual footprints of the universality of these dominant coherent small-scale structures.

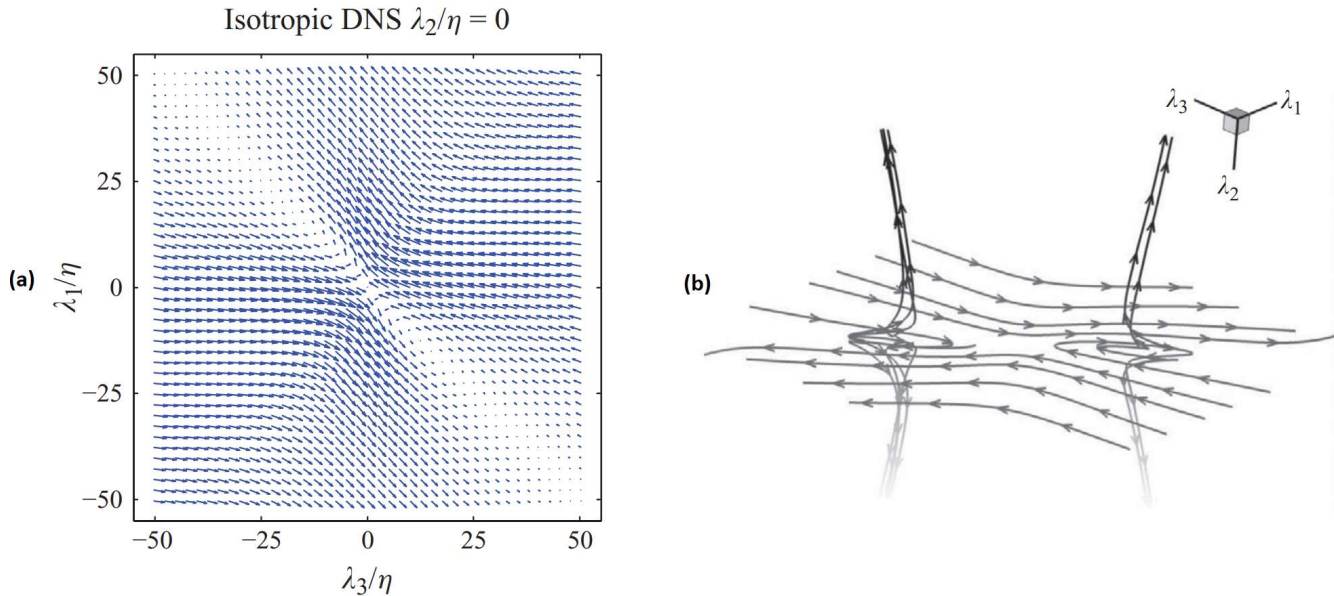


Fig. 1 (a) Average velocity pattern on a plane defined by the first and third eigenvector of the strain rate tensor for points in DNS of isotropic turbulence, shown as velocity vectors in the $\vec{\lambda}_1 - \vec{\lambda}_3$ and (b) the corresponding average Eulerian 3D streamlines (Elsinga and Marusic 2010)

Referring to the view of (Elsinga et. al. 2017), the fact that the average shear layer dimensions are consistent with instantaneous results obtained by DNS (Ishihara et. al. 2013) confirms that they are not an artifact induced by the averaging procedure but show a key feature of instantaneous turbulent flows. In this contribution we present the progress of the development of algorithms to answer three questions.

- How do the universal structures form and disappear?
- Which role do the universal structures play in the energy dissipation process?
- What are the properties of the particle tracks when they pass through such a (conditioned) universal structure?

To answer these questions time resolved data of a von Kármán flow obtained by a dense Lagrangian Particle Tracking Technique is used. The photograph and a sketch of the set-up at the GTF3 of MPI, Göttingen is shown in Figure 2 (for details see Schröder et al. 2022). Table 1 shows the experimental parameter settings with various time series of snapshots at two different particle image densities aiming at full convergence of Lagrangian particle statistics and the Eulerian velocity vector, respective velocity gradient tensor and pressure fields statistics. First, a 3D camera

calibration based on a two-sided two-plane target from LaVision, volume-self-calibration (VSC) (Wieneke 2008) and the estimation of the particles Optical Transfer Function (OTF) for each camera and sub-volume (Schanz et al. 2013) has been processed. Then the STB algorithm (Schanz et al. 2016) with recursive application of the IPR method (Wieneke 2013, Jahn et al. 2021) has been applied to the series of time-resolved images from the four high-speed cameras. A two-pass STB approach was employed, which first tracks forwards in time, then reverses the image order and elongates existing tracks backwards in time, while reconnecting possible track-fragments. The particle tracks (up to $\sim 80,000$ per time step and measurement volume for the high seeding cases) have been stored and a temporal filter using 3rd order B-splines has been applied with optimal weighting coefficients derived from the cross-over frequency between signal and noise of the particle tracks-position spectrum (Gesemann et al. 2016). The filtered particles positions and the calculated analytical temporal derivatives, velocities and acceleration information are used as input for the above mentioned data assimilation method FlowFit. In addition to the evaluation of large amounts of Lagrangian particle track data with relatively little computational power by STB, the subsequent application of FlowFit (Gesemann et al. 2016) data assimilation using position, velocity and acceleration data along all tracks as input offers the computation of the time-resolved full velocity gradient tensor (VGT) $A = \nabla \vec{v}$ and pressure fields $\bar{p} = \frac{p}{\rho}$ on arbitrary points without numerical interpolation. The cell size of the individual 3rd order cubic B-Splines is chosen to be $\sim 300 \mu\text{m}$ corresponding to $\sim 2.7\eta$ and $\sim 4.8 \eta$ for the two Reynolds numbers, respectively. A slice of a single time step of the resulting FlowFit data for $Re_\lambda = 370$ is shown in Figure 3. In the following only the higher Reynolds number is considered.

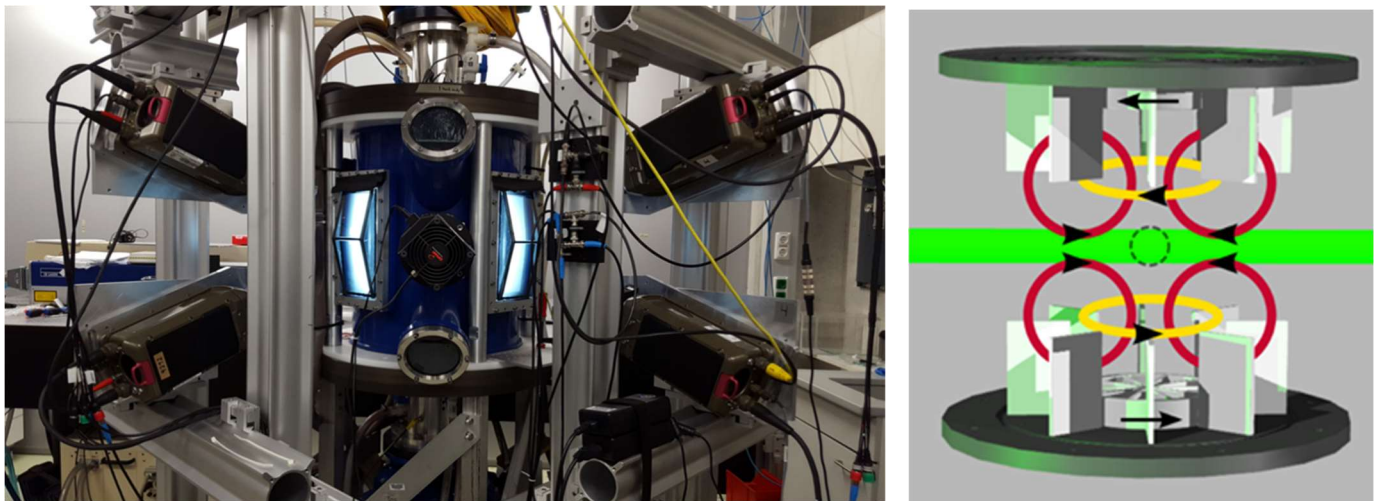


Fig. 2 Experimental set up-with four 4 Mpx high speed cameras (v640) for dense Lagrangian Particle Tracking inside the GTF 3 facility at the MPI-DS, Göttingen using Shake-The-Box (left). The turbulent Kármán flow at $Re_\lambda = 370$ is produced with two counter-rotating disks with impellers following the principle sketch (right)

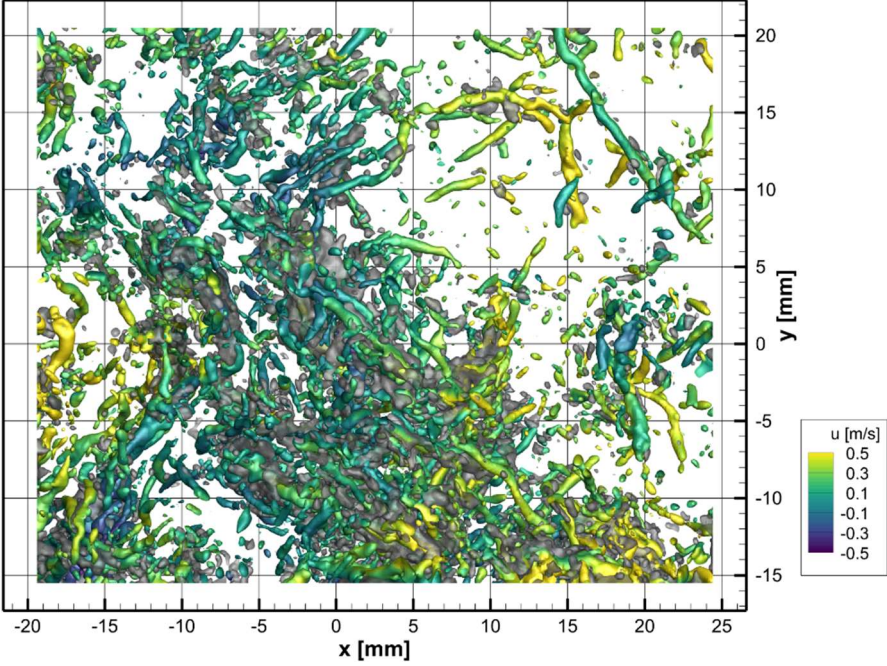
Flow properties	$\tau_\eta \sim 3.93\text{ms}$	
	$\eta = 61.8\mu\text{m}$	
	$Re_\lambda \sim 370$	
Camera parameters	1280 x 1200 px	
	3.33 kHz ($<1/13\tau$)	
Statistics (lower seeding)	1000 x 200 imgs	
	2000 x 40 imgs	
Spatiotemporal structures (high seeding)	3 x 14000 imgs (1000τ)	
Volume	40 x 40 x 15 mm ³ (670 x 670 x 250 η^3)	

Table 1 Experimental parameter of the STB campaign using the propeller rotation frequency $f = 1\text{Hz}$ at $Re_\lambda = 370$ and related flow properties of the Kármán flow facility GTF 3, including recent findings on the dissipation rate. (left)

Fig. 3 Slice of FlowFit data, iso-surfaces of Q-criterion, $Q = 7000\text{ s}^{-2}$ color coded by x-component of velocity and grey iso-surfaces at $\epsilon = 6.5 \cdot \langle \epsilon \rangle$ from FlowFit (right).

Furthermore, the strain rate tensor S , the local energy dissipation rate $\epsilon = 2\nu S S$ as well as the enstrophy $\nu\omega^2$ and the principal invariants of incompressible flow $Q = \text{tr}(A)$ and $R = -\det(A)$ can be determined. The main limitation is the underestimation of the velocity derivatives due to the low pass filtering effect caused by the mean 3D particle distance of $\sim 9\cdot\eta$, so that despite using optimized spatial interpolation with physical regularization by the FlowFit procedure, this leads to an underestimated mean energy dissipation rate of $\langle \epsilon \rangle_{FF} = 0.041 \frac{\text{m}^2}{\text{s}^3}$. Therefore, the computation of the flow properties shown in Table 1 is based on an estimation of $\langle \epsilon \rangle = 0.063 \frac{\text{m}^2}{\text{s}^3}$ using a statistical velocity/acceleration structure function approach which is valid for the (well resolved) inertial subrange (Falkovich 2012, Jucha 2014, Schröder 2022). However, the (coarse grained) dissipation evaluation using FlowFit is possible on every single point in the measurement domain, and is therefore used for estimating instantaneous values. Despite the mentioned low-pass-filter effects high energy dissipation rate or enstrophy events can be detected for the well sampled energy containing structures and used for further Eulerian and Lagrangian statistics assuming that the underlying “true” velocity gradients would consist of even higher amplitudes.

Another advantage of the STB/FlowFit approach is the presence of particle tracks embedded within the time-resolved (coarse grained) velocity gradient tensor and pressure fields which allow us to include the Lagrangian view to obtain a more complete picture of the coherent structures. Therefore, we can present the coherent structures in connection with the properties of the tracer particle tracks resp. fluid elements forming them.

2. Methodology

We search for instantaneous realizations of the dominant foci-saddle point pattern hereinafter referred to as “events”, to obtain the time evolution of the coherent structures in the strain rate tensor eigenframe. In order to achieve this an algorithm is necessary, which consists of a detection and a tracking procedure.

The detection procedure is based on the original algorithm described in Elsinga and Marusic 2010 and is briefly summarized as follows:

- (1) Compute the eigenvectors of the strain rate tensor of a random point in the measurement volume.
- (2) Change the sign of the second eigenvector if its direction does not coincide with the vorticity vector.
- (3) Change the sign of the first eigenvector to maintain a right-handed coordinate system if necessary.
- (4) Sample the velocity and dissipation in the local coordinate system defined by the eigenvectors $\vec{\lambda}_i$ of S .
- (5) Transform the properties into the eigenframe.
- (6) Save the event if the maximum of topology strengths components $d_i = \min_j \left(\frac{\vec{\lambda}_2 \circ \vec{\omega}_{ij}}{|\vec{\omega}_{ij}|} \right)$ with vorticity $\vec{\omega}_{ij}$ in one of the expected vortex pair positions i (distance to the origin) and j (quadrant) shown in Figure 4 being higher than the threshold. The evaluation of topology strength is performed using three different vortex pair positions since the distance between the vortices and the origin decreases with increasing dissipation (Elsinga et. al. 2017).

Steps (2) and (3) are necessary to avoid averaging out the expected structure, such that the averaged event would only show a pure strain pattern.

With Taylor’s frozen-flow assumption these events can be tracked in time using the velocity in the middle of the structure to find the position of the event in the following time step. To determine the position of the event more precisely, the advection velocity is not used directly. Instead, the

advection velocity defines the size of a box described by 27 grid points enclosing the position of the event in the previous time step. Among these positions the one with the highest structure strength is selected as midpoint of the event in the current time step. This position is then used to sample the velocity and dissipation in its respective eigenframe. The change of direction of the vorticity vector in a time coherent event can not change to the opposite direction in the time period ($<1/13\tau_\eta$) between to particle images. Therefore, the signs of the eigenvectors $\vec{\lambda}_i$ are adjusted such that they point roughly in the same direction as the eigenvectors of the previous time step. This ensures that the strain rate tensor eigenframe rotation is a representation of the rotational movement of the event. Before averaging, the event tracks are shifted in time in such a way that the time step with the highest topology strength is considered as $t = 0$. Thus, the average strength is strongest at $t = 0$, so that all time steps before can be interpreted as the formation of the event, while time steps thereafter show its decay. To reduce the influence of measurement inaccuracies, a low pass filter is applied on the sequence of structure strengths before evaluating its maximum. The positions of event tracks at $t = 0$ can then serve as a starting point for a second tracking procedure, in which the events are advected forward and backward in time. The tracking procedure can also be used for other kind of events by giving the structure strength d another meaning. An interesting application for this is the tracking of highly dissipative events by defining the structure strength as a local average of dissipation.

To answer the third question raised in the introduction, flow regions with high energy dissipation rates are identified. Particle tracks passing through those regions (a box with edge length 19.5η around the maxima) are gathered ($\sim 200,000$) and their Lagrangian and Eulerian (and pressure) properties are averaged along the particle tracks or fluid elements for each time-step to get insight in the related (mean) energy exchange process. The same method using enstrophy as structure strength allows the investigation of Lagrangian tracks ($\sim 100,000$) passing through the area of such events.

3. Event tracking results

If random points are used as the basis for the averaging procedure, the known foci-saddle point structure emerges, as shown in Figure 4. Thus, the universal structure can be detected not only in DNS and Tomo PIV data (Elsinga and Marusic 2010), but also in STB/FlowFit data of turbulent flows. The conditioning on high dissipation causes the foci to be closer together, which is in good agreement with the averaged shear layer computed by Elsinga et. al. 2017.

Furthermore, the average velocity is much higher in Figure 4b, suggesting that the average event originate primarily from locations with high dissipation.

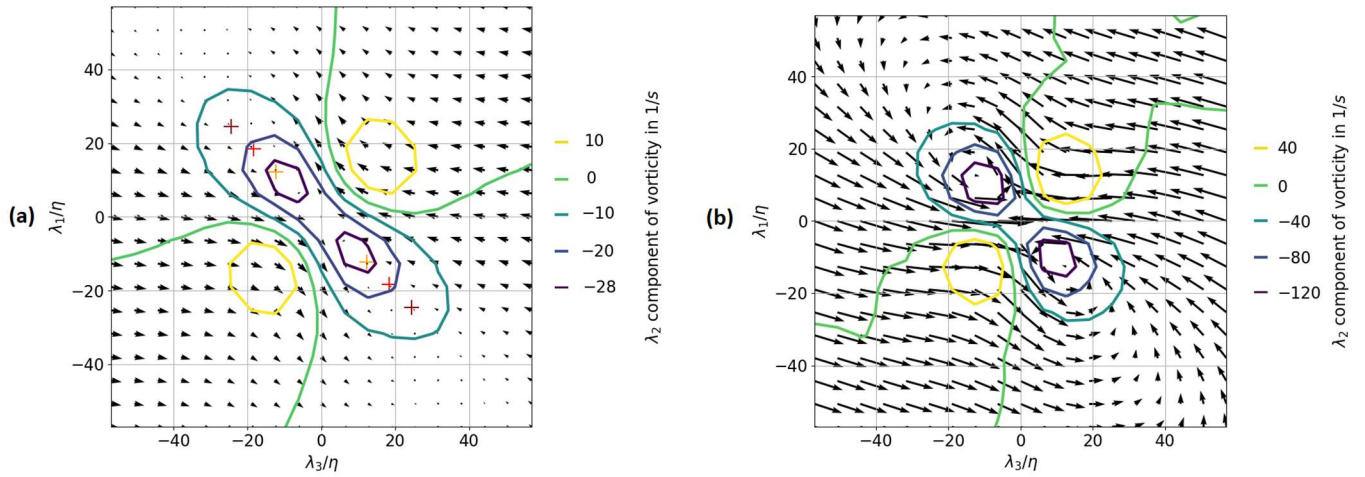


Fig. 4 Average velocity pattern on a plane defined by the first and third eigenvector of the strain rate tensor for every event (a) with three vortex pair positions (plus symbols) considered for the evaluation of topology strength. The same average pattern is observed by conditioning on dissipation $\epsilon > 7.5\langle\epsilon\rangle$. (b) The scaling between arrow size and velocity is the same for both figures.

Using the event detection with a structure strength threshold $d_{min} = 0.95$ on the spatiotemporal dataset shown in Table 1, events with high structure strength can be found. Elsinga and Marusic conjectured, that the pattern is not only an averaging artifact, but shows instantaneous structures characterising turbulent behaviour. If this is true and the detection algorithm is able to find the events, the average of velocities without using high structure strength locations must not show the pattern. As can be seen in Figure 5, the pattern formed by averaging without events of high structure strength do not show the foci-saddle point structure. This fact supports the assumption of Elsinga and Marusic and shows that the algorithm is able to find the events.

The rotation rate of the strain rate eigenframe and the vorticity at the origin of the tracked events should be similar as long as the structure remains stable. In order to verify the functionality of the tracking procedure, probability density functions of both values for all tracked events are shown in Figure 6. This indicates that although the distributions of both properties are quite similar, the rotation is occasionally very high. This is to be expected due to the existence of decaying events, which are accompanied by structure topology changes.

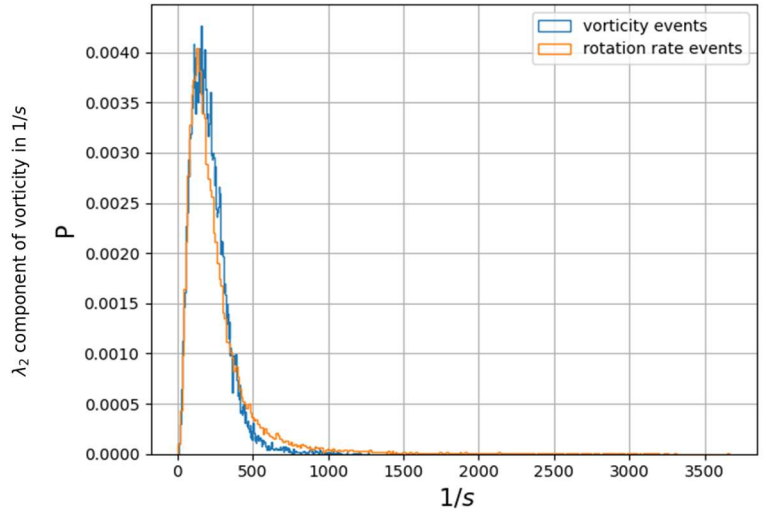
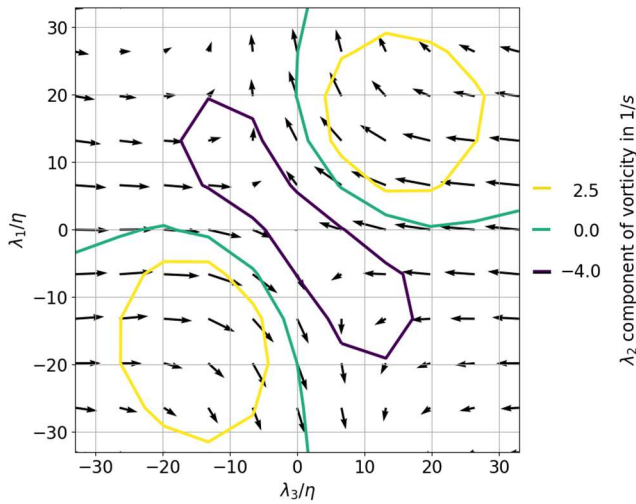


Fig. 5 Ensemble average of locations with structure strength $d < 0.5$.

Fig. 6 PDF of strain eigenframe rotation rates and vorticity in tracked events.

The average tracked event sampled on 11×11 points at $t = 0$ with mean structure strength of $d_{t_0} = 0.99$ is shown in Figure 7. The coherent structure is clearly visible, but the node-saddle topology is less pronounced than in the event shown in Figure 4a. The dissipation maximum is located in the middle of the event. The dissipation rate level over the whole plane is smaller than the (underestimated) average $\langle \epsilon \rangle_{FF} = 0.041$, which indicates that high dissipation events in particular hardly seem to meet the required alignment between vorticity and $\vec{\lambda}_2$, which prevents their identification. The pressure distribution shows two minima, as expected considering the vorticity iso-contour lines shown in Figure 4a.

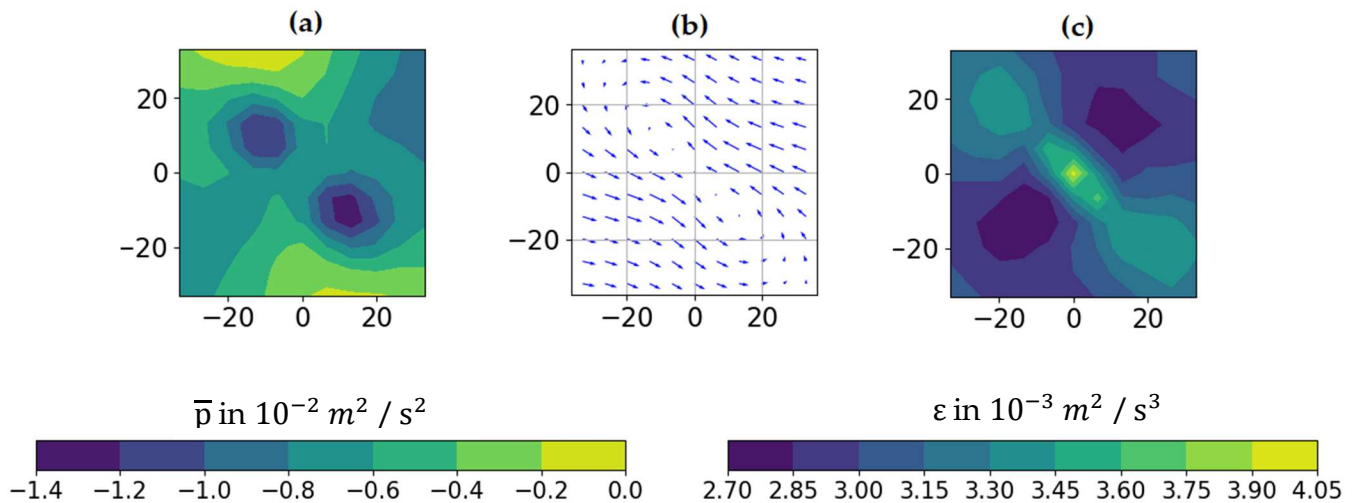


Fig. 7 Average pressure pattern (a), velocity pattern (b) and dissipation pattern (c) in the $\vec{\lambda}_1 - \vec{\lambda}_3$ eigenplane using 111,598 tracked events.

Although instantaneous universal small scale structures exist and contribute significantly to the mean structure, the tracked events are individually very different in the distribution of pressure, dissipation, and velocity. Therefore, the results are not fully converged even with the high number of 111,598 events tracked. In addition, many events can only be tracked over a short period of time, so that only 11,717 elements are available averaging on timestep $t = -3\tau_\eta$.

The problem also exists when tracking events with decreasing structure strength, so that at $t = 3\tau_\eta$ only 16,462 events remain. Despite the fact that tracking of Eulerian structures like strong vortices proved to work well (Elsinga et al. 2012), the events were found to vary much in their topology over time. One reason for the fragility of the tracked events may be the chosen structure strength definition, which detects mostly structures with weak vorticity. However, it is also possible that this type of structure actually has a short lifespan, as the two vortices are only in close proximity to each other for a short time.

4. Lagrangian Tracks statistics

Highly dissipative events contribute particularly to the universal structure velocity distribution, as can be seen in Figure 4b. Therefore we now deal with the statistics of particle tracks passing through or close by high dissipative events. In addition, high enstrophy events are also examined for comparison.

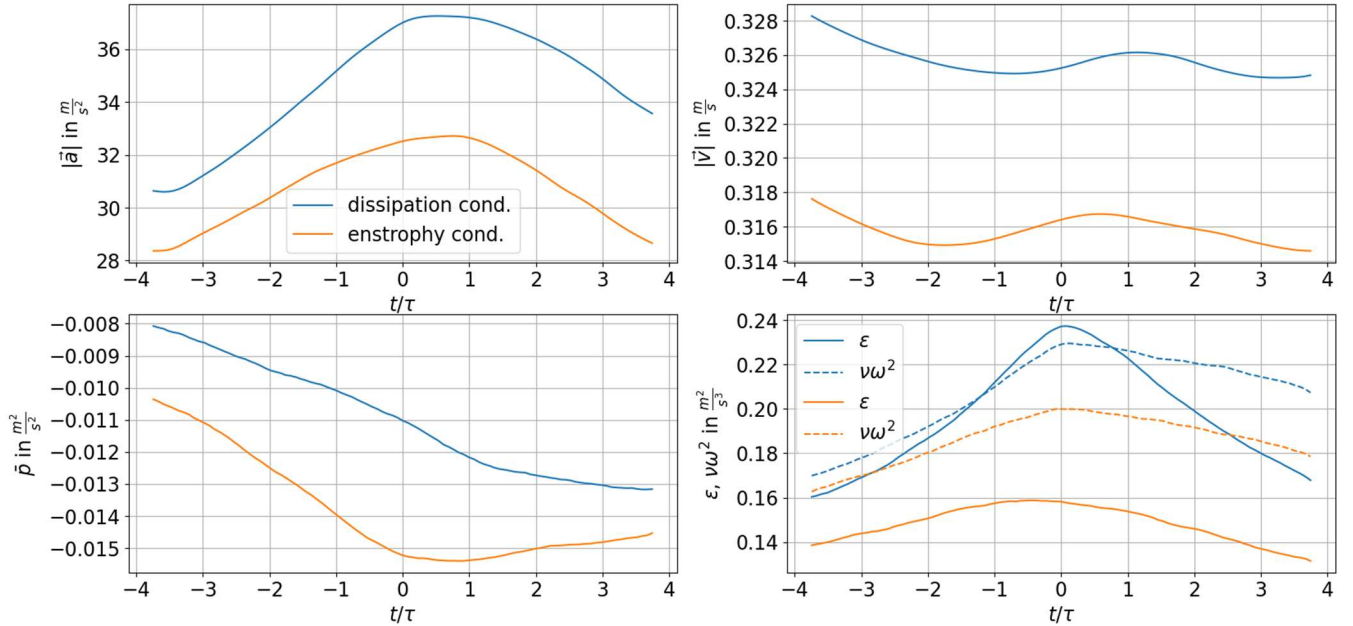


Fig. 8 Ensemble average of acceleration and velocity magnitude, pressure, dissipation and enstrophy for each time step for particle tracks passing through a box of high dissipation locations ($\epsilon > 7.5(\epsilon)$) or high enstrophy locations ($\nu\omega^2 > 7.5 < \nu\omega^2 >$) respectively from 4τ backward to 4τ forward in time. Box size: $19.5\eta \times 19.5\eta \times 19.5\eta$

The mean acceleration, velocity, pressure, dissipation and enstrophy of particle tracers passing through a box with 19.5η edge length containing such events are shown in Figure 8. Due to the conditioning, the tracks are statistically independent although the data set contains only about 2000 time series. For the representation of velocity and acceleration, only the particle data are necessary. The remaining quantities require velocity gradients or pressure which are derived from the FlowFit field at the respective particle track positions backward and forward in time. The plots show that local acceleration and velocity maxima are reached after the dissipation maximum. The pressure decrease slows down after this time, while the enstrophy reaches its maximum at $t = 0$, and then falls only slowly. This could be an indication for the temporal transition of the Lagrangian particle surrounding topology from a node-saddle- to a vortex structure topology, in a mean sense. The dissipation maximum is smaller than the threshold for finding the high dissipation event, because of the large box size used for gathering the particle tracks. The energy exchange processes within certain structures consist of the sum of the Lagrangian particle tracks that form them. Thus, linking Lagrangian tracks to the Eulerian structures they pass through gives us a direct insight into the energy exchange processes of various structures. The time course of Lagrangian particle tracks in terms of the power balance equation

$$\vec{a} \cdot \vec{v} = \nu \Delta \vec{v} \cdot \vec{v} - \nabla \bar{p} \cdot \vec{v} \quad (1)$$

and of the viscous transport term

$$T = \nu \Delta \vec{v} \cdot \vec{v} + \varepsilon \quad (2)$$

as well as of the Q-value in a mean sense during the time-span from $-4\tau_\eta < t_0 < 4\tau_\eta$ is shown in Figure 9.

Since the results shown open up a new view of the energy exchange processes, the following interpretations are only a first attempt to get an idea of the processes involved.

The $\vec{a} \cdot \vec{v}$ plot shows a drop, which starts shortly after passing the high dissipation event and lasts a little longer than $2\tau_\eta$. During this time T drops below zero, indicating a power flow into a new flow structure, while the Q-value rises. The term $\nu \Delta \vec{v} \cdot \vec{v}$ is strongly negative all the time, which shows how important the viscous term is in highly dissipative events. These results and the picture of the universal structure occurring in turbulence shown in Figure 1 point out the following scenario. Fluid particles stemming from coherent bulk flow regions with opposite velocity directions approach each other creating high velocity gradients in a shear layer resulting in high energy dissipation events and a decrease of their power. The resulting Kelvin-Helmholtz instability provides for a small scale motion which is reflected in the formation of a pressure minimum in vicinity to the strong shear event. A part of the power of the particles flow into the formation of a vortex, as the rising Q-value indicates.

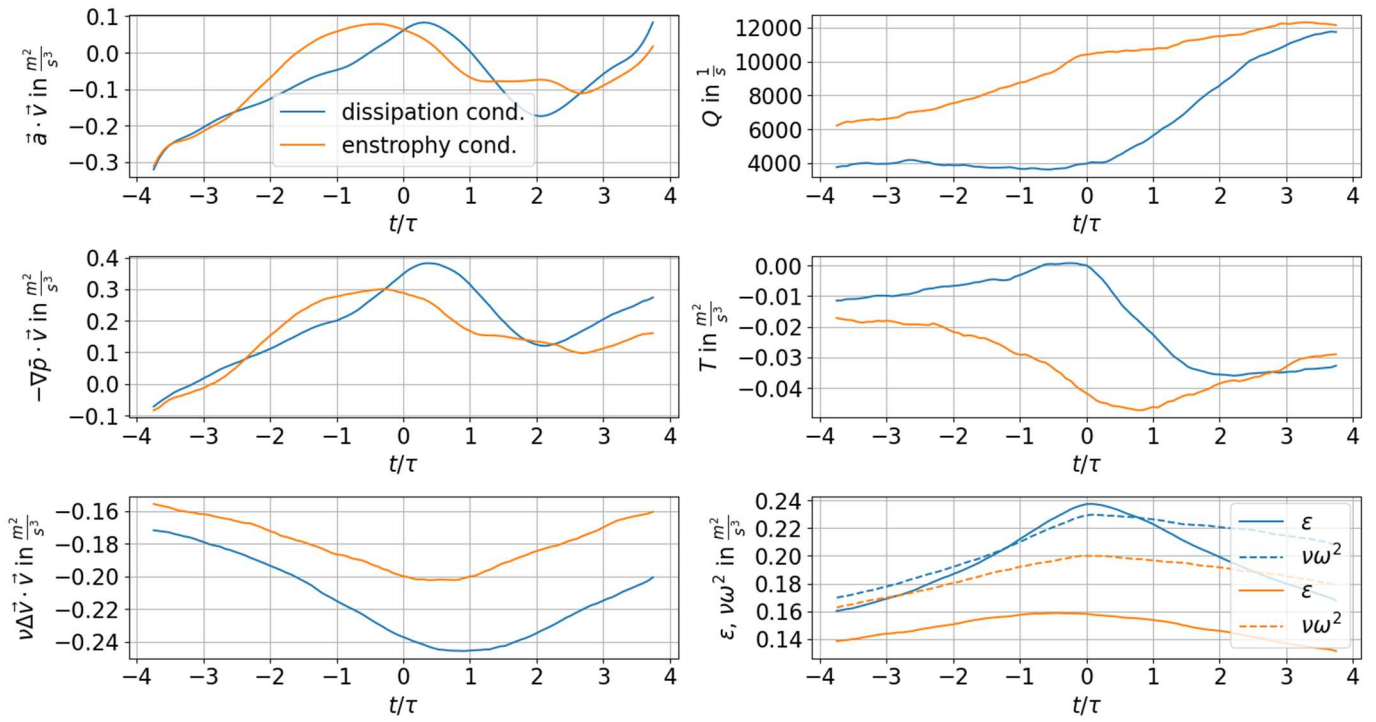


Fig. 9 Ensemble average of each term in the energy balance equation and the viscous energy transport , Q-value as well as enstrophy and dissipation for each time step from 4τ backward to 4τ forward in time for particle tracks passing through a of high dissipation locations ($\epsilon > 7.5(\epsilon)$) or high enstrophy locations ($v\omega^2 > 7.5 < v\omega^2$) respectively. Box size: $19.5\eta \times 19.5\eta \times 19.5\eta$.

In this process the transfer into high dissipation therefore not only leads to an energy sink (production of heat) but also an upscaling in form of vorticity. Particles sucked into the newly formed vortex begin to accelerate and leave the structure. Particle tracks leading through regions of high enstrophy, on the other hand, show a resembling decrease in power even though they have lower velocity and acceleration values. The high power before passing an event with high enstrophy is therefore an indication of an alignment of acceleration and velocity, which is to be expected in pressure gradient driven events.

A visual representation of particle tracks forming an instantaneous high dissipation event can be seen in Figure 10. For the display, an event was tracked, and every particle in a box placed around the position of the event at a point in time was gathered. The positions of the tracks corresponding to the particles are visualized relative to the dissipation event origin in its timestep. The tracks shown, like the mean properties, indicate that the origin of the highly dissipative event is a bulk flow region. Taking into account the fact that the power before the event is low and the pressure decreases during the approach, one can conclude that bulk flow events from different directions, which collide through a pressure minimum into a common point, are responsible for particularly high dissipation events.

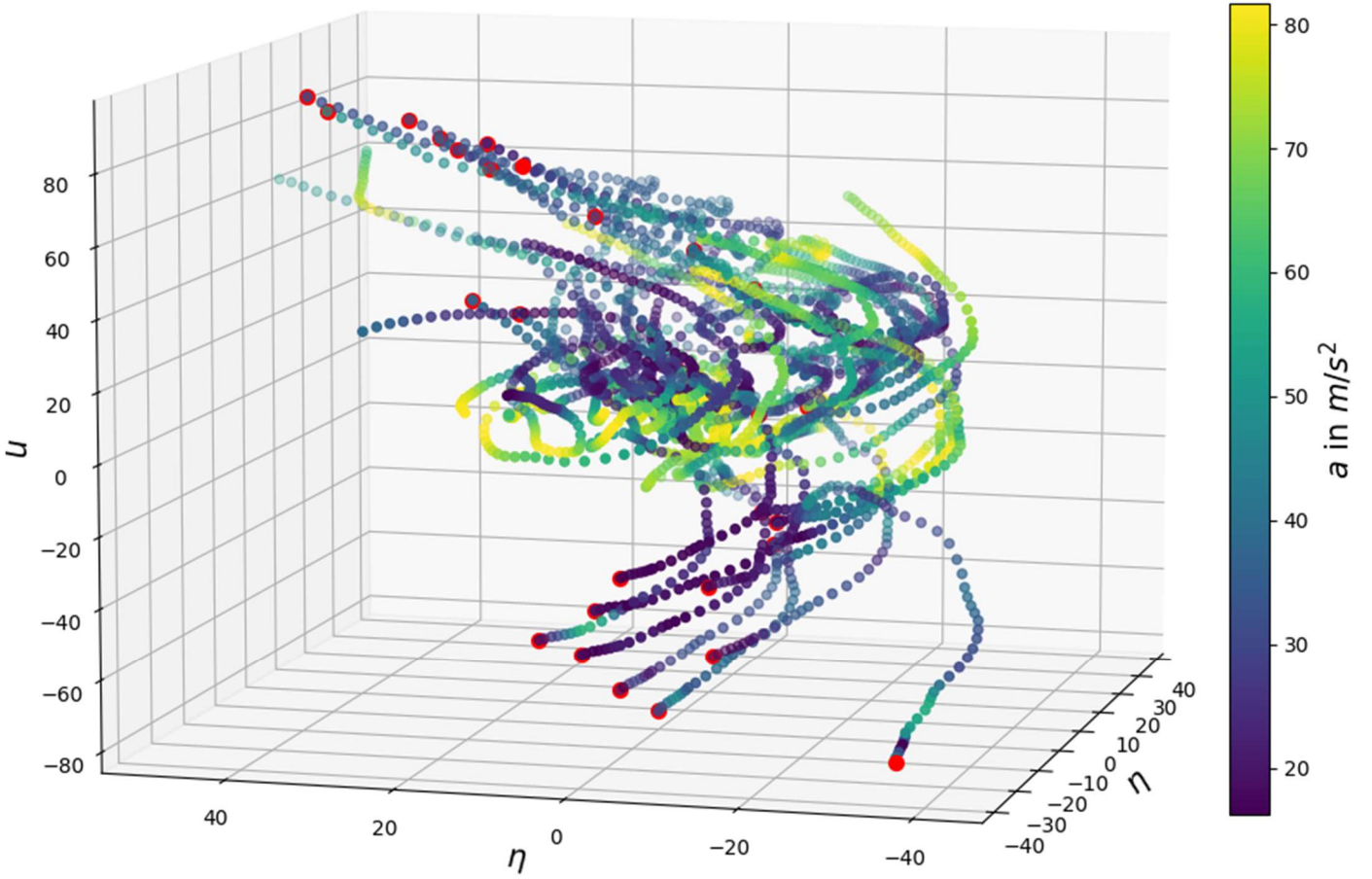


Fig. 10 Instantaneous particle tracks passing through a dissipation event. Red dots indicate the beginning of a particle track. Box size $19.5\eta \times 19.5\eta \times 19.5\eta$.

5. Summary and Conclusions

In this contribution velocities sampled in their respective strain rate eigenframes were averaged using experimental data of a von Kármán flow with $Re_\lambda = 370$. We have found the same foci-saddle point structure identified as a universal small scale feature as in previous experiments and DNS (Elsinga and Marusic 2010). Furthermore, an approach to track the universal structure to investigate its properties over their lifetime was presented. As a measure of structure strength the minimum of alignments of the second eigenvector of the strain rate tensor and the vorticity located in the expected vortex positions was used. The ensemble average of velocity of these events showed a pattern which resembles the universal structure.

It has been shown that the averaged event contains two pressure minima at the vortex positions, while there is a dissipation maximum at the origin. The dissipation averaged over the whole $\vec{\lambda}_1 - \vec{\lambda}_3$ eigenplane is smaller than the average dissipation, which indicates that the detection algorithm primarily finds weak events. The events were tracked forwards and backwards in time using Taylor's frozen-flow assumption in combination with a shaking approach. With the current

algorithm, only $\sim 15\%$ of the events are tracked more than $3\tau_\eta$ using their highest structure strength as reference, which means that most of the events either have a small lifetime or the tracking approach is not suitable for this kind of structure.

To investigate universal properties also in the Lagrangian perspective, we gathered particles leading to intermittent events using dissipation or enstrophy respectively as structure strength. The mean properties of the tracks through highly dissipative events show how particles from opposing bulk flow regions approach each other and not only energy is converted into heat, but also upscaling in the form of vorticity is generated.

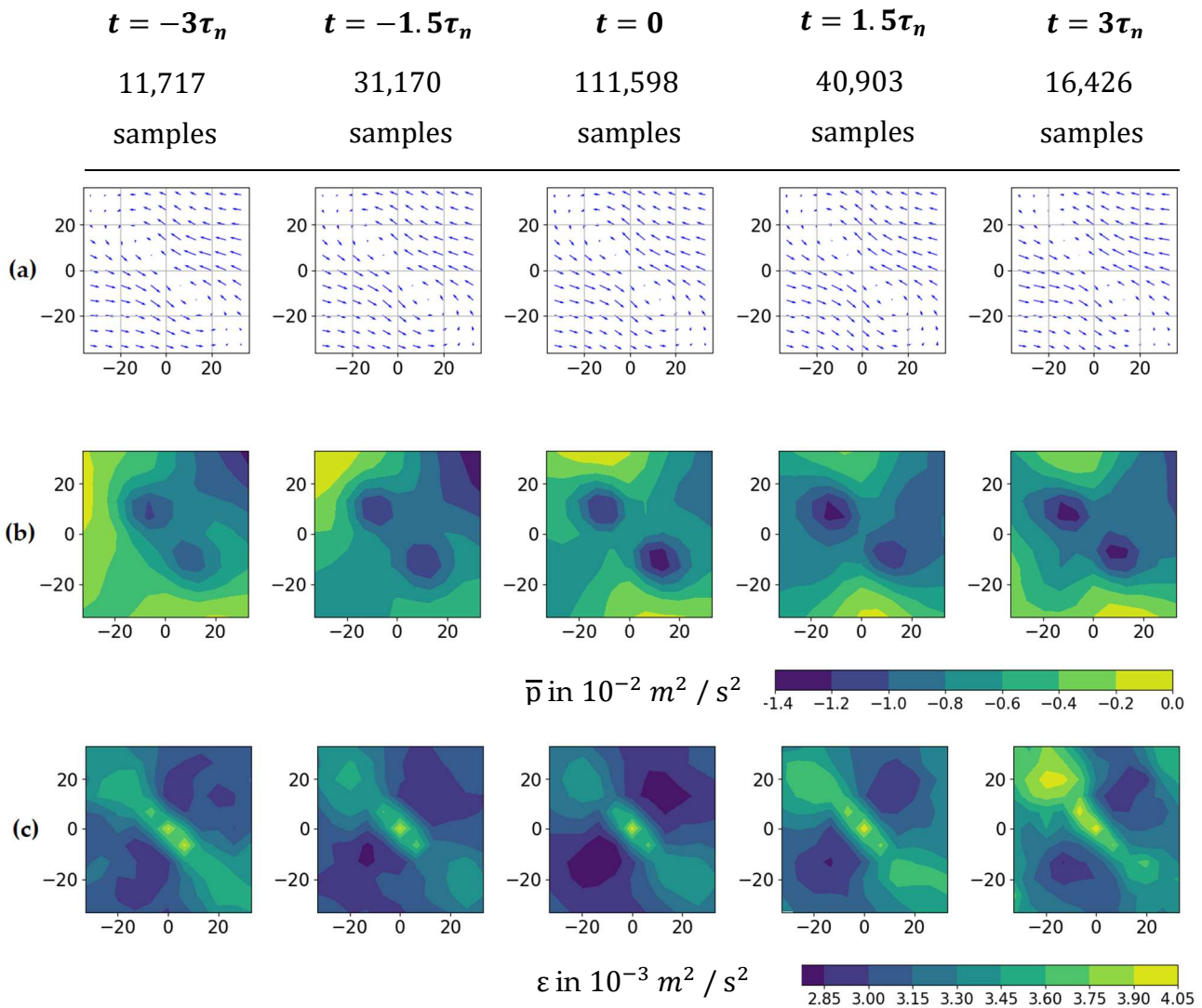


Fig. 11 Time sequence of the average velocity (a), pressure (b) and dissipation (c) pattern in the $\vec{\lambda}_1 - \vec{\lambda}_3$ eigenplane using 111,598 tracked events.

6. Outlook

The time tracking of events with structure strength as defined in this contribution leads to a lack of statistical convergence as can be seen in Figure 11, because most of the events are very short. In order to answer the question of the longevity of the universal structure, adjustments to the tracking approach presented here are necessary. One possibility would be to use the vorticity projected onto $\vec{\lambda}_2$ instead of using just their alignment. In addition to the universal events, the tracking of extreme dissipation and enstrophy locations is also worthwhile. Each of these approaches would benefit from using mainframe capacities. This would allow a denser as well as a three-dimensional sampling of the tracked structures. The study of properties of the lagrangian tracks would also benefit from the use of more computing power. This would allow a joint analysis of R and Q values on particle tracks through extreme events longer than those presented in this work. From this analysis it could be concluded from which topologies such events arise and into which topologies the involved particles are guided.

7. Acknowledgement

We acknowledge funding from the European High-Performance Infrastructures in Turbulence (EuHIT) consortium for the DTrack measurement campaign and the support of the staff at MPI-DS in Göttingen. Computer resources for this project have been provided by the Gauss Centre for Supercomputing/Leibniz Supercomputing Centre under grant: pr62zi. We acknowledge Eberhard Bodenschatz from MPI-DS for his support and John Lawson for his cooperation during the set-up of the high-speed laser at the MPI-GTF3 facility. We thank Prof. G.E. Elsinga for his suggestion to establish a time tracking approach for the universal structure.

8. References

- Chong, M.S., Perry, A.E., & Cantwell, B.J. (1990), A general classification of three-dimensional flow fields, *Phys. Fluids A* 2, 765
- Elsinga, G. E., Poelma, C., Schröder, A., Geisler, R., Scarano, F., & Westerweel, J. (2012), Tracking of vortices in a turbulent boundary layer. *Journal of fluid mechanics*, 697, 273-295.
- Elsinga, G.E., & Marusic, I. (2010), Universal aspects of small-scale motions in turbulence, *Journal of Fluid Mechanics*, 662, 514–539
- Elsinga, G.E., Ishihara, T., Goudar, M.V., da Silva, C.B., & Hunt, J.C. (2017), The scaling of straining motions in homogeneous isotropic turbulence, *J. Fluid Mech*, 829, 31-64

Falkovich G, Xu H, Pumir A, Bodenschatz E, Biferale L, Boffetta G, Lanotte A S and Toschi F (2012), On Lagrangian single-particle statistics. *Phys. Fluids* 24, 055102

Gesemann, S., Huhn, F., Schanz, D., & Schröder, A. (2016), From Noisy Particle Tracks to Velocity, Acceleration and Pressure Fields using B-splines and Penalties, 18th Lisbon Symposium, Portugal

Ishihara, T., Kaneda, Y., Hunt, J.C. 2013 Thin shear layers in high Reynolds number turbulence – DNS results. *Flow Turbul. Combust.* 91, 895–929.

Jahn, T., Schanz, D. & Schröder, A. (2021), Advanced iterative particle reconstruction for Lagrangian particle tracking. *Exp Fluids* 62, 179. <https://doi.org/10.1007/s00348-021-03276-7>

Jucha, J. (2014), Time-Symmetry Breaking in Turbulent Multi-Particle Dispersion, Dissertation, <http://hdl.handle.net/11858/00-1735-0000-0023-98F1-4>

Kolmogorov A.N. (1941), Dissipation of energy in locally isotropic turbulence, *Dokl. Akad. Nauk SSSR* 32(1). English translation in *Proc. R. Soc. Lond. A* (1991) 434, 15–17

Schanz, D., Gesemann, S., & Schröder, A. (2016), Shake The Box: Lagrangian particle tracking at high particle image densities, *Exp. Fluids* 57:70

Schanz, D., Gesemann, S., Schröder, A., Wieneke, B., & Novara, M., (2013), Non-uniform optical transfer function in particle imaging: calibration and application to tomographic reconstruction, *Meas Sci Technol* 24, 024009

Soria, J., Sondergaards, R., & Cantwell, B.J., A study of the fine-scale motions of incompressible time-developing mixing layers, *Physics of Fluids* 6, 871

Schröder, A., Schanz, D., Gesemann, S., Huhn, F., Paz, D.G., & Bodenschatz, E. (2022), Measurements of the energy dissipation rate in homogeneous turbulence using dense 3D Lagrangian Particle Tracking and FlowFit, 20th Lisbon Symposium, Portugal

Tsinober, A. (2001), *An Informal Introduction to Turbulence*, Kluwer

Wieneke, B. (2008), Volume self-calibration for 3D particle image velocimetry, *Exp. Fluids* 45:549–556

Wieneke, B. (2013), Iterative reconstruction of volumetric particle distribution, *Meas. Sci. Technol* 24, 024008